Journal of Clinical Periodontology
Official Journal of The European Federation of Periodontology
Founded by the British, Dutch, French, German, Scandinavian, and Swiss Societies of Periodontology

J Clin Periodontol 2009; 36: 265–277 doi: 10.1111/j.1600-051X.2008.01363.x

Journal of Clinical Periodontology

Early healing of implants placed into fresh extraction sockets: an experimental study in the beagle dog. De novo bone formation

Fabio Vignoletti[1], Carina Johansson[2], Tomas Albrektsson[3], Massimo De Sanctis[4], Fidel San Roman[5] and Mariano Sanz[1]

[1]Universidad Complutense de Madrid, Periodoncia, Madrid, Spain; [2]Department of Clinical Medicine, School of Health and Medical Sciences, Örebro University, Örebro, Sweden; [3]Department of Biomaterials/ Handicap Research, Sahlgrenska University Hospital, Institute for Surgical Sciences, University of Gothenburg, Gothenburg, Sweden; [4]Dipartimento di Scienze odontostomatologiche, Università degli Studi di Siena, Siena, Italy; [5]Universidad Complutense de Madrid, Veterinaria, Madrid, Spain

Vignoletti F, Johansson C, Albrektsson T, De Sanctis M, San Roman F, Sanz M. Early healing of implants placed into fresh extraction sockets: an experimental study in the beagle dog. De novo bone formation. J Clin Periodontol 2009; 36: 265–277. doi: 10.1111/j.1600-051X.2008.01363.

Abstract

Objectives: Describe the early phases of tissue integration in implants placed into fresh extraction sockets and test whether a new implant surface nano-topography (DCD nano-particles, Nanotite™) promotes early osseointegration when compared with minimally rough surface implants (DAE, Osseotite®).

Material and Methods: Sixteen beagle dogs received 64 test and control implants randomly installed into the distal socket of $_3P_3$ and $_4P_4$. Histomorphometric analysis of bone to implant contact (BIC) and bone area was performed at 4 h, 1, 2, 4 and 8 weeks.

Results: Wound healing initiated with a coagulum that was substituted by a provisional matrix at 1 week. Bone formation started concomitant to a marked bone resorption. At 2 weeks, woven bone formation was evident and gradually remodelled into lamellar bone at 4 and 8 weeks. BIC increased similarly throughout the study in both groups with a tendency to higher percentages for the test devices at 2 and 4 weeks. The influence of the DCD nano-particles was more evident at the fourth premolar site.

Conclusion: Osseointegration occurred similarly at both implant groups, although the socket dimension appeared to influence bone healing. It is suggested that the enhanced nano-topography has a limited effect in the immediate implant surgical protocol.

Key words: implant surface; osseointegration; fresh extraction socket; nanotopography; animal models

Accepted for publication 20 November 2008

Introduction

Different types of implant systems have been used to replace missing teeth, including subperiosteal implants, endosseous implants with fibrous encapsulation and endosseous implants with direct bone-to-implant contact (BIC). Only the latter have demonstrated long-term predictable success due to the bone-to-implant interface termed *osseointegration*, defined as the direct contact between living bone and a load-carrying implant (Albrektsson et al. 1981, Schroeder et al. 1981). In order to reach osseointegration, the implant must attain, when introduced in the bone bed, proper primary stability and other adequate healing conditions leading to bone formation until reaching the direct BIC. This biological process has been studied in different experimental animal models. Berglundh et al. (2003) designed an experimental wound chamber with the aim of allowing the evaluation of bone healing from 2 h to 3 months after implant installation. Using this model these authors have described the sequence of biological events that starts with the formation of a coagulum between the hard tissue bed and the implant surface until dense lamellar bone lays in direct contact with the implant surface. After 1 week of healing, the coagulum is replaced with granulation tissue containing mesenchymal cells, matrix components and newly formed vessels. At 2 weeks, a cell-rich immature bone (woven bone) begins to surround the blood vessels and starts to get in contact with the titanium surface. Between 2 and 4 weeks of healing, the newly formed mineralized bone extends from the cut bone ends and covers most of the implant surface. During the subsequent weeks, these trabeculae of woven bone are replaced with mature bone and after 6–12 weeks

Conflict of interest and source of funding statement

The authors declare that they have no conflict of interests.
This study was partially sponsored by a research grant from Biomet 3i.

of healing, most of the area of the bone-to-implant interface is filled with mineralized dense lamellar bone (*osseointegration*). This process of bone modelling and remodelling will continue, although at a slower rate, providing increased resistance to shear forces, still 1 year or more after implant placement (Johansson & Albrektsson 1987).

Studies evaluating improvements in implant surfaces have demonstrated that changes in the surface microtopography enhance bone healing after implant placement and, thus, the use of implants with so-called moderately rough surfaces would achieve fast and predictable osseointegration (Wennerberg et al. 1995, 1996a, b, c). Recently, studies from these authors have investigated how changes at nano-scale level of the implant surface may further enhance bone response in vivo in a rabbit model (Meirelles et al. 2007, 2008a, b). In these studies, the authors used hydroxyapatite and titania nano-particles to modify smooth titanium implant surfaces. These preliminary results have been corroborated with human studies (Goene et al. 2007, Orsini et al. 2007) in which a new implant surface characterized by discrete crystalline depositions (DCDs) of nanometer-scale calcium phosphate (CaP) particles on a dual acid-etched implant surface (DCD nano-particles, Nanotite™ Biomet 3i) was compared with a standard dual acid-etched surface (DAE, Osseotite® Biomet 3i). These human histological results showed a significant enhancement of bone response during the early stages of healing around implants placed in poor-quality bone.

Improvements of the implant surface microtopography have been paralleled with the development of surgical approaches aimed to reduce the healing time and to provide enough primary stability to achieve osseointegration and thus allowing the early functional loading of the implants. One of these proposed surgical approaches is the immediate placement of implants into fresh extraction sockets, with the aim to reduce healing time and to improve the bone-to-implant congruence. Experimental investigations have shown that osseointegration occurs predictably with this surgical approach (Anneroth et al. 1985, Todescan et al. 1987, Barzilay et al. 1991). Moreover, clinical studies have reported similar survival rates and similar histological findings with implants placed in healed ridges, at least with short-term follow-ups (Schropp et al. 2003). Recent animal studies investigating the healing process of implants placed into fresh extraction sockets have, however, demonstrated significant ridge alterations occurring 1–3 months after implant placement, with marked vertical and horizontal resorption of the buccal alveolar crest (Araujo et al. 2005, 2006a, b, Rimondini et al. 2005, Botticelli et al. 2006), being this healing significantly different when compared with implants placed in healed ridges (Botticelli et al. 2006). In spite of these findings, we are still lacking knowledge on the early stages of healing and the long-term clinical outcomes of this surgical protocol. Hence, the purpose of this experimental investigation is to study in detail the biological sequence of healing during the early phases of tissue integration when implants are placed into fresh extraction sockets. Further this study aims to describe how implants with identical geometry but with a different surface nano-topography (DAE *versus* DCD nano-particles) may influence these biological events.

Materials and Methods

Sample

This experimental animal study was carried out at the Experimental Surgical Centre of the Hospital ''Gomez-Ulla'' in Madrid, Spain, once the *Regional Ethics Committee for Animal Research* approved the study protocol.

The sample consisted on 16 female adult beagle dogs with a weight between 10 and 20 kilograms and a mean age of 1.5 years. Throughout the experimental study, the animals were kept on a soft diet and subject to oral hygiene by mechanical cleaning of both teeth and implants using a toothbrush and toothpaste.

Study device

The implants utilized had the geometry of commercially available Osseotite-Certain straight-walled implants with a diameter of 3.25 mm and 8.5, 10 and 11.5 mm long. Control implants had a dual acid-etched surface (DAE, Osseotite®, Biomet 3i) while in the test implants their surface was modified by the deposition of discrete crystals of CaP, which superimposes a nano-scale surface topography upon an already complex microtopographic titanium surface produced by acid etching (DCD nano-particles Nanotite™, Biomet 3i). This proprietary, so-called DCD, is achieved by immersing the metallic implants in a suspension of CaP crystals, ranging in size between 20 and 100 nm and resulting in approximately 50% of the metallic surface being covered by the crystals with the remaining surface being metal oxide (Mendes et al. 2008). Test implants were visibly indistinguishable from control implants. All implants had an internal abutment connection into which healing abutments were adapted.

Surgery

Once the animals were sedated with a cocktail containing 80 μg/kg of Medetomidine (Domtor®, Pfizer, Madrid, Spain), 20 μg/kg of Butorfanol (Torbugesic®, Fort Dodge, Gerona, Spain) and 100 μg/kg of Atropine Sulphate (Atropina®, Instituto Farmacéutico FAS, Burgos, Spain), they were placed under general anaesthesia with a mixture of sevofluorane 2 l/h (Sevorane®) and oxygen using a mechanical respirator throughout the surgery.

Once anaesthetized, buccal and lingual intra-sulcular incisions were performed from the mesial of the third premolars $_3P_3$ to the mesial of the first molars 1M1 on both sides of the mandible. Muco-periosteal full thickness flaps were reflected on both sides just to disclose the marginal aspect of the ridge in order to facilitate the tooth extraction. The third and fourth mandibular premolars ($_3P_3$ and $_4P_4$) on both sides were hemisected with the use of a diamond cylindrical bur under copious irrigation and then both roots were removed with the use of forceps and osteotomes. The extraction was carefully executed to preserve the integrity of the socket walls. The distal socket of each premolar (3P and 4P) was chosen as the study site while the mesial sites were allowed to heal without intervention, thus providing 4 study sites per dog (Fig. 1a and b).

Based on the amount of available bone measured with a periodontal probe (North Carolina probe, Hu-Friedy, Germany) on the extracted root, the implant osteotomies were drilled. The drilling sequence used was the 2.0 and 2.75 mm twist drills to the expected depth of the osteotomy and a final 3.0 mm diameter drill through only the coronal half of the osteotomy. Osteotomies were cut to ensure that the implant seating platform was levelled

with the buccal crestal margin. Test and control implants were randomly assigned to the distal sockets of $_3P_3$ and $_4P_4$ on each side of the mandible using a computer generated random list. Once the implants were inserted and primary stability was attained, the healing abutments were screwed to the fixtures and the mucoperisostal flaps were replaced and secured with resorbable interrupted sutures (Vicryl® 4.0) (Fig. 2a and b). Dogs were then fed with a soft diet and their teeth were regularly cleaned, every third day, with a 0.12% clorohexidine solution sprayed on their teeth.

Experimental design

The experimental protocol and timing between implant installation and biopsy is depicted in Table 1. Five healing periods were evaluated: baseline (2 h) and 1, 2, 4, and 8 weeks post-implant installation. Because each animal provided four study implant sites and three animals were included at each of the five healing periods, 12 implants and abutments (six test and six control) were studied at each healing period. One extra animal was available to replace any animal that had to be excluded from the study for health or other reasons.

Animal sacrifice

At each allocated healing period, the animals were sacrificed with an overdose of sodium pentothal and perfused through the carotid arteries with a fixative solution (Karnovsky 1965). The mandibles were freed from their attachment tissues, cut in half sections and placed in the Karnovsky fixative/preservative solution. The solution comprised 20 g of paraformaldehyde, 250 ml of distilled water, 100 ml of glutaraldehyde and 150 ml of 0.2 M PBS (pH 7.2), for 500 ml of fixative solution (Karnovsky 1965).

Histological processing

The specimens were dehydrated in graded series of ethanol and embedded in LR White resin (London Resin Company, Berkshire, UK) and were prepared for ground sectioning according to methods described by Donath & Breuner (1982). The block biopsies were cut in a bucco-lingual plane using a cutting–grinding unit (Exakt® Apparatebau, Norderstedt, Germany). From each implant site, one central bucco-lingual section was prepared and further

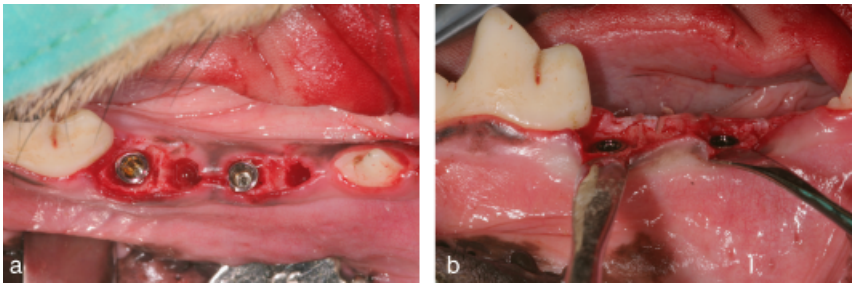

Fig. 1. Implants in the right side of the mandible immediately after installation: (a) occlusal view, 433 × 288 mm (180 × 180 DPI); (b) buccal view. 433 × 288 mm (180 × 180 DPI).

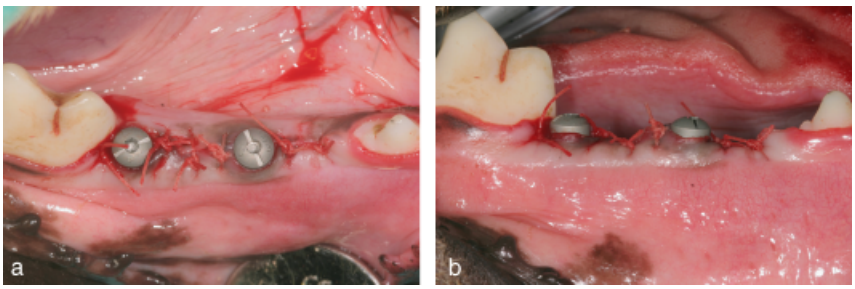

Fig. 2. Implants after the healing abutments were secured and flaps were sutured: (a) occlusal view, 433 × 288 mm (180 × 180 DPI); (b) buccal view. 433 × 288 mm (180 × 180 DPI).

Table 1. Study schedule. Each group provided 3 animals (group 5, 8 weeks included 4 animals)

Groups	– 1 week	Baseline	1 week	2 weeks	3 weeks	4 weeks	7 weeks	8 weeks
Group 5 8 weeks	Profylaxis	Surgery						Biopsy
Group 2 1 week		Profylaxis	Surgery	Biopsy				
Group 3 2 weeks			Profylaxis	Surgery		Biopsy		
Group 4 4 weeks					Profylaxis	Surgery		Biopsy
Group 1 4 h							Profylaxis	Surgery Biopsy

Each animal provided four study sites, 2 tests and 2 controls.
677 × 381 mm (72 × 72 DPI).

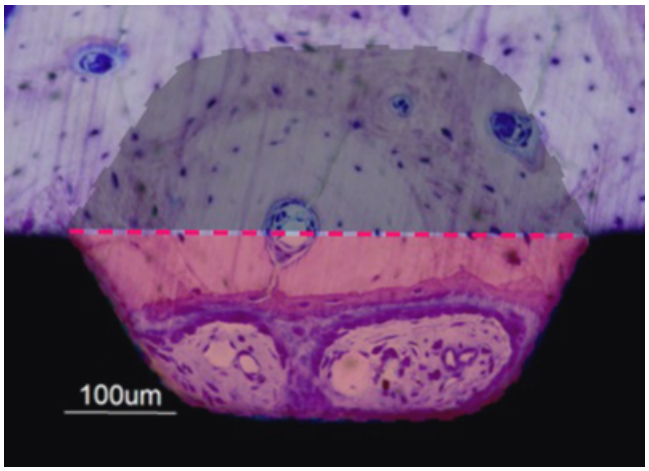

Fig. 3. Wound chamber provided by the device. Figure shows the two areas of interest: thread area (red) and marginal mirror area (black). 101 × 141 mm (72 × 72 DPI).

reduced to a final thickness of about 20 μm by microgrinding and polishing using a microgrinding unit (Exakt® Apparatebau). The sections were stained in toluidine-blue.

Histological evaluation

The histological evaluation was performed directly in the eyepiece of a Leitz Aristoplan Light Microscope equipped with a microvid and coupled to a PC for direct computer-based measurements. All measurements were made with a 10 × objective and a 10 × eye piece. Four bucco-lingual sections per animal were investigated. All sections were examined in a blind manner. Digital micrographs were obtained using a digital camera connected to the microscope.

Two histological evaluations were carried out. The first was a histometric study evaluating the main quantitative outcome measurement that was the linear *BIC*. BIC was calculated along the entire length of the implant in mean percentages assessed both from (i) the buccal and (ii) the lingual side of the implant and expressed as a mean of buccal and lingual side.

The second histological evaluation was the morphometric analysis that allowed for the quantification of two outcome variables. First, we measured the bone area as the mineralized tissue fraction (percentage of mineralized tissue). Secondly, we quantified the newly formed bone, distinguishing between parent bone, *new mineralized tissue*, bone remnants and non-mineralized tissue.

Both outcome variables were evaluated in the wound chamber and the reproduced specular mirror area. The significance of the reflected image of the screw thread area in the adjacent bone has been reported by Johansson (1991). Figure 3 depicts the landmarks delimiting these spaces.

Because the socket dimensions of the third and the fourth premolar are different (Araujo et al. 2005, Blanco et al. 2008), the results from both the histometric and morphometric measurements were further observed after stratifying for socket location. We then described the results at the wider distal socket of the fourth premolar $_4P_4$ and at the narrower mesial socket of the third premolar $_3P_3$, thus assessing whether a wider gap between the implant surface and the bony walls had any influence on the histological outcome.

Data analysis

The dog was used as the statistical unit of analysis; thus for each variable a mean value for each implant group and animal has been calculated and used for the data analysis. Histological results were expressed in mean percentages (± SD). Comparisons between test/control implants and among the different healing periods/groups were analysed using the two-way ANOVA. The Bonferroni post hoc analysis was further performed to evaluate for significance among the different time intervals. Differences were considered statistically significant when p was <0.05. This statistical analysis was performed using the software Prism 5.0 (GraphPad, San Diego, CA, USA). Because of the limited number of dogs and implants per group, when the data were stratified by socket location, the statistical analysis was carried out comparing the outcomes of the third and fourth premolar sites, without further dividing into test and control groups according to the differential implant. These results of test and control groups at third and fourth premolar sites are just presented in a descriptive manner.

Results

Histometric analysis

Primary outcome: bone-to-implant contact

The degree of osseointegration was evaluated by measuring the changes in linear BIC from baseline (4 h after implant placement) to 8 weeks (Table 2).

Results from histometric measurements of BIC showed a very similar pattern of osseointegration for test and control implants throughout the entire study (Fig. 4). Four hours after implant placement, the BIC was mostly limited

Table 2. Table shows results from histometric measurements (mean (SD)) of bone to implant contact (BIC)

B.I.C.	DAE	Statistics	DCD nanoparticles	Statistics
4 h	14.9 (7.5)		11.7 (7.5)	
1 week	5.2 (1.4)		6.4 (1.5)	
2 weeks	10.5 (9.4)		13.1 (13.0)	
4 weeks	26.0 (19.0)		29.0 (14.2)	
8 weeks	45.7 (18.8)		42.4 (21.5)	

677 × 381 mm (72 × 72 DPI).

P < 0.05
P < 0.01
P < 0.001

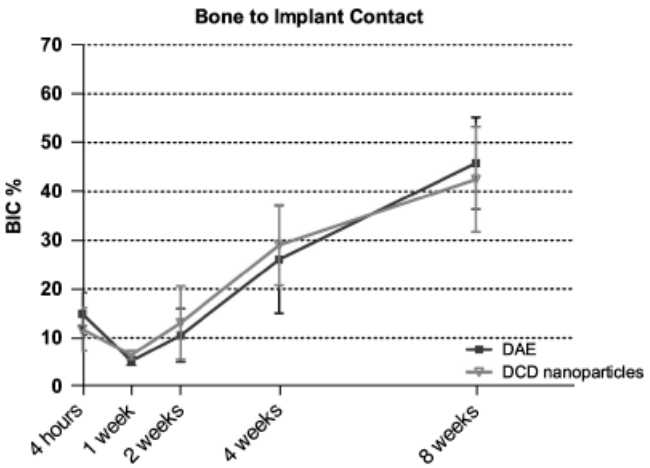

Fig. 4. Degree of osseointegration (BIC%) from 4 h to 8 weeks at the DCD nano-particles (red) and DAE (blue) devices. BIC%, bone-to-implant contact percentage. 167 × 136 mm (300 × 300 DPI).

to the thread tip level and amounted to 14.9% and 11.7% for the control (DAE) and test implants (DCD nano-particles), respectively. At 2 weeks the BIC ranged from 4.5% to 21.4% with a mean value of 10.5% (SD 9.4%) in the controls, while in the tests it ranged from 5.5% to 28.1% with a mean 13.1% (SD 13.0%), thus demonstrating higher BIC percentages at the test implants, although these differences were not statistically significant. At 4 weeks the results were similar for the two surfaces with an overall mean percentage of BIC of 26.0% (SD 19.0) and 29.0% (SD 14.2), respectively. At 8 weeks the BIC% gradually increased to 45.7% (SD 18.8) for the control and to 42.4% (SD 21.5) for the test implants.

When all implants were grouped and results were compared according to implant location ($_3P_3$ *versus* $_4P_4$), the outcomes were similar demonstrating a linear increase in BIC percentages in both sockets (Fig. 5). However, when we assessed the independent behaviour of test and control implants stratified by socket location, the differences between the two implant surfaces were more pronounced. While the third premolar site evidenced similar healing dynamics between both groups throughout the entire experiment (Fig. 6a), the fourth premolar site demonstrated higher BIC percentages at 2 and 4 weeks for the test implants (Fig. 6b). In this site, BICs at 2 weeks were 11.7% (SD 3.1) and 22.7% (SD 9.9) for the control and test implant groups, respectively, and at 4 weeks, 28.7% (SD 18.1) and 43.4% (SD 6.2), respectively.

Morphometric analysis

Figure 7 illustrates the relative proportions of lamellar bone, new mineralized tissue, bone remnants and non-mineralized tissue for each time point. At 4 h after implant placement, the histological image at the thread level was similar for both implant surfaces. The interior of the wound chamber was occupied by non-mineralized tissue, mainly composed of erythrocytes and in smaller proportions, old bone and bone chips remnants from the drilling (Fig. 8a and b). Remnants of the periodontal ligament attached to the bundle bone were occasionally observed (Fig. 9a and b). At this healing time, the relative proportions of non-mineralized tissue, parent bone and bone chips were 63.3% (SD 9.6), 34.8% (SD 8.3) and 0.9% (SD 1.0) for the

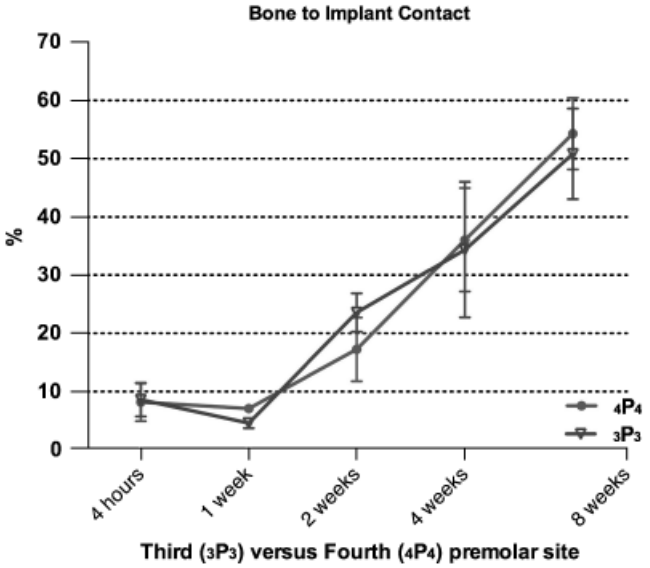

Fig. 5. Degree of osseointegration (BIC%) from 4 h to 8 weeks at the fourth premolar site (green) and at the third premolar site (purple). BIC%, bone-to-implant contact percentage. 143 × 136 mm (300 × 300 DPI).

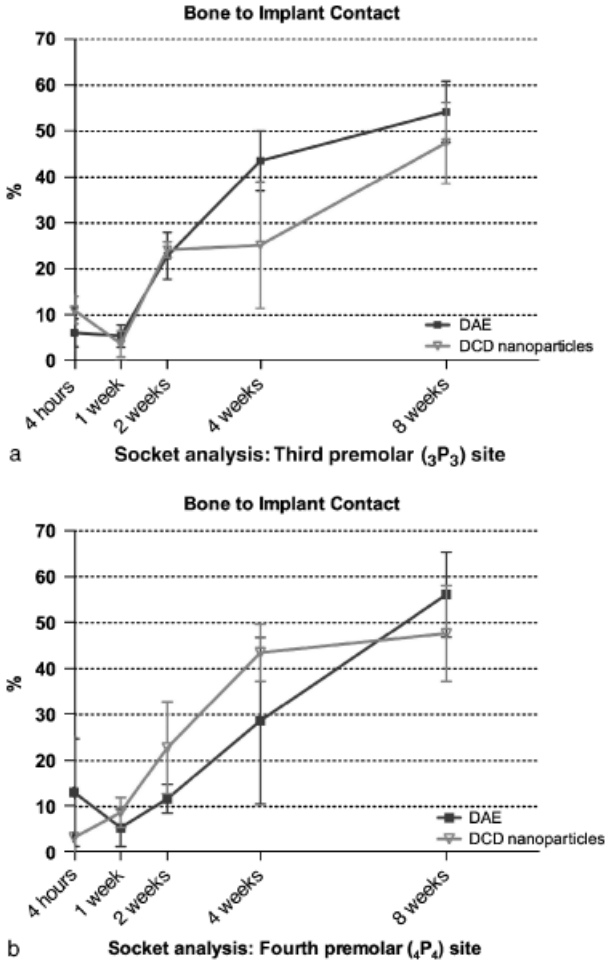

Fig. 6. Degree of osseointegration (BIC%) from 4 h to 8 weeks at the DCD nano-particles (red) and DAE (blue) devices: (a) third premolar site. BIC%, bone-to-implant contact percentage; 165 × 148 mm (300 × 300 DPI); (b) fourth premolar site. BIC%, bone-to-implant contact. 168 × 148 mm (300 × 300 DPI).

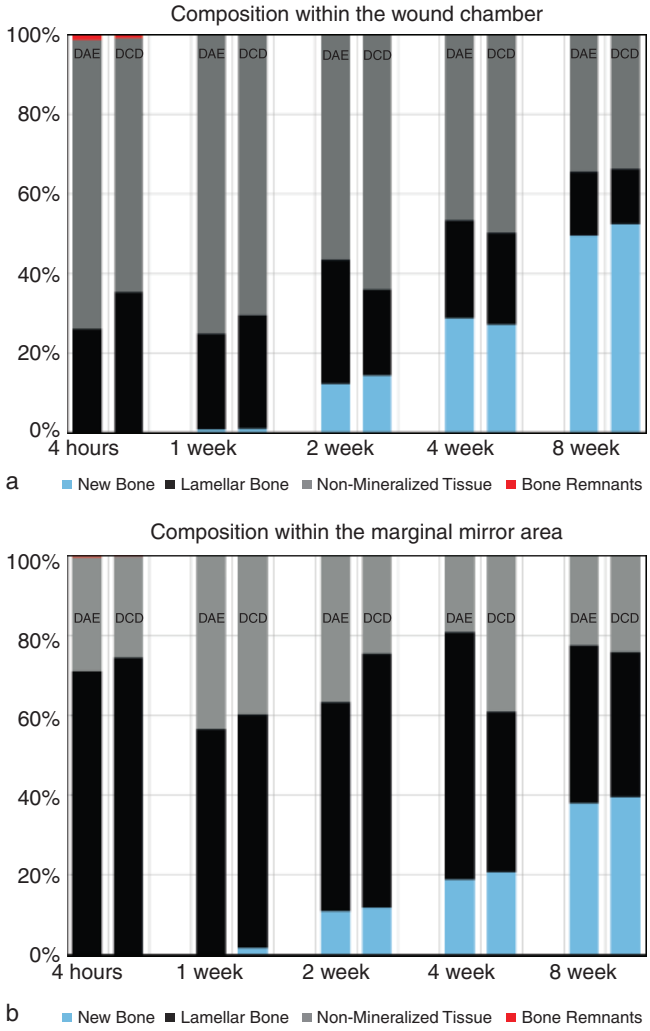

Fig. 7. Histograms showing the results of the morphometric analysis of the ground sections. Assessments were performed at 4 h, 1, 2, 4 and 8 weeks after implant placement. Proportions of woven bone, lamellar bone, non-mineralized tissue and bone remnants in the (a) wound chamber and (b) marginal mirror area. DAE, control surface; DCD, test surface. 677 × 381 mm (72 × 72 DPI).

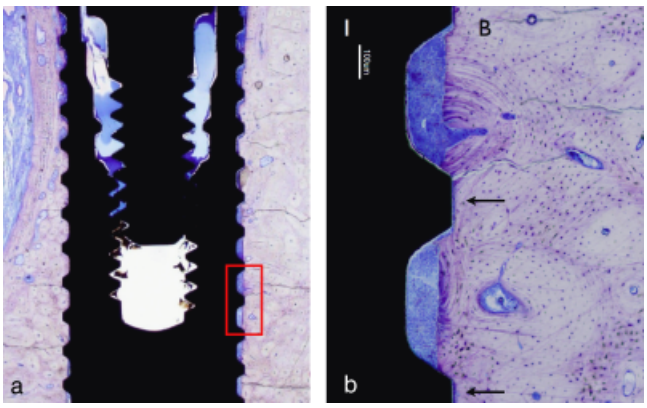

Fig. 8. (a) Implant with surrounding tissues after 4 h of healing. Toluidine-blue staining. Original magnification × 10. (b) Detail of (a). A coagulum is interposed between the implant surface (I) and the parent bone (B). Thread tips (arrows) in close contact with bone tissue. Toluidine-blue staining. Original magnification × 16. DAE surface. 677 × 381 mm (72 × 72 DPI).

control and 72.6% (SD 9.9), 26% (SD 8.9) and 1.4% (SD 1.3) for the test implants, respectively.

At 1 week, the wound chamber was mainly filled with granulation tissue, rich in fibroblast-like cells within a fibrin-like extracellular matrix. This soft tissue portion occupied 70.8% (SD 4.9) and 75.2% (SD 9.6) of the thread for control and test implants, respectively. At this time interval, the bone modelling process was absent, with minimal traces of new bone formation, mainly representing woven bone formation, in percentages of 0.9% (SD 1.3) and 0.7% (SD 1.0) of the threaded area for control and test specimens, respectively. Areas of bone remodelling were observed in the parent bone (Fig. 10a and b).

At 2 weeks, bone modelling was manifest, with woven bone formation clearly identifiable in both groups. The histological results observed in both implant surfaces were similar. In the test group, the proportion of woven bone had increased from 0.7% (SD 1.0) at 1 week to 12.2% (SD 9.0) at 2 weeks. New bone formation (Fig. 11a–c) was observed both in intimate contact with the surface (contact osteogenesis or de novo bone formation), as well as adjacent to the old parent bone (distance osteogenesis, Fig. 10) (Davies 1998). A marked angiogenesis, paralleled to the osteoblastic activity, was noticeable (Fig. 12a and b). New bone formation represented 14.2% (SD 7.7) of the tissue in the thread area of the chamber in the control implants.

At 4 weeks, both bone modelling and remodelling events were observed. The new bone formation represented a mixed of woven bone and a parallel-fibred bone, clearly distinguishable from the old parent bone by a reverse cement line (Fig. 13a and b). The amount of new bone formation increased to 27.0% (SD 8.1) in the control and 28.7% (SD 5.0) in the test implants.

At 8 weeks, the histological picture of the thread area was very similar for control and test implants. 66.3 (SD 9.9)% and 65.5% (SD 3.4) of the thread area was respectively occupied by bone. In the new bone portion, areas of woven bone were mixed with parallel-fibred bone as well as with mature lamellar bone, representing 52.3% (SD 3.2) and 49.4% (SD 3.2) of the thread, respectively (Fig. 14a and b).

The results from the morphometric measurements of bone area (mineralized

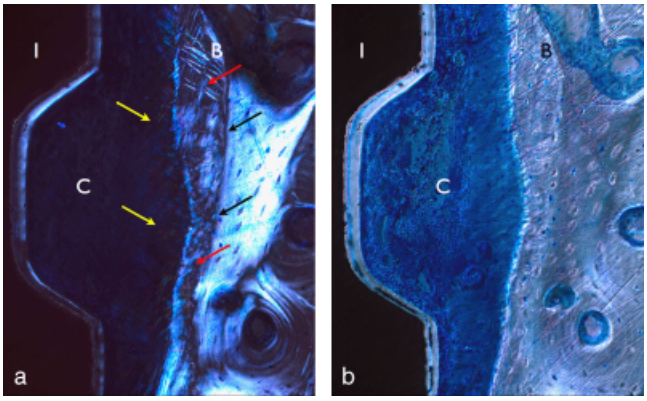

Fig. 9. Ground section representing 4 h healing interval. Wound chamber filled with a coagulum (C) that is interposed between the implant surface (I) and the bone tissue (B). Note the remnants of the periodontal ligament (yellow arrows) attached to the bundle bone (red arrows). Cement line separates the bundle bone from the parent bone (black arrows): (a) polarized light, (b) interference contrast. Toluidine-blue staining. Original magnification × 40. DAE surface. 677 × 381 mm (72 × 72 DPI).

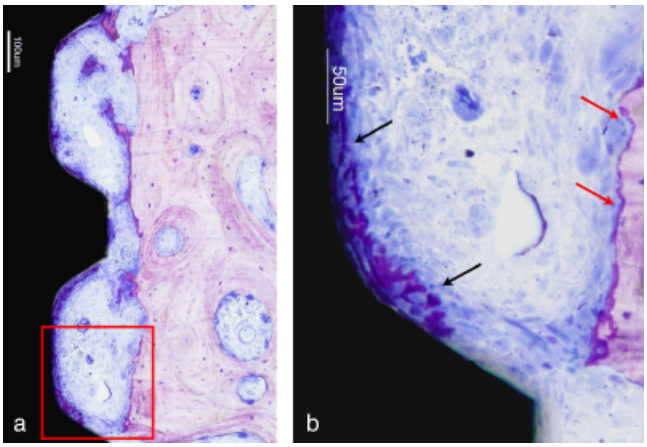

Fig. 10. (a) Section representing 1 week healing interval. Provisional matrix of connective tissue cells with first signs of bone formation (dark stained area). Ground section. Toluidine-blue staining. Original magnification × 16. (b) Detail of (a). Woven bone in intimate contact with the implant surface (contact osteogenesis) (black arrows). Areas of bone remodelling observed in the parent bone (red arrows). Toluidine-blue staining. Original magnification × 40. DCD nano-particles.

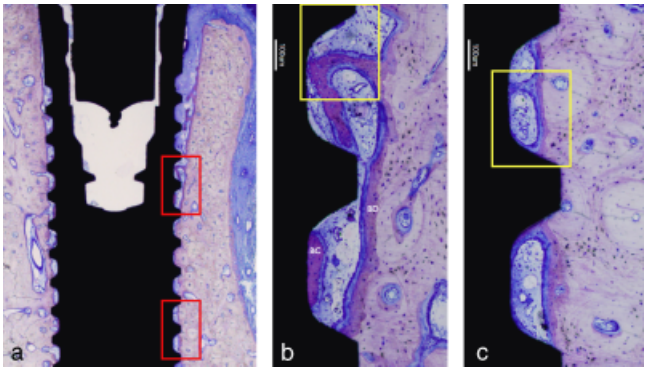

Fig. 11. (a) Implant with surrounding tissues after 2 weeks of healing. Dark stained areas indicate evident woven bone formation in the surrounding tissues. Original magnification × 10. (b) Detail of (a). Woven bone formation continuous with the parent bone (distance osteogenesis, BD) and along the surface of the implant (contact osteogenesis, BC). Inset: Fig. 12. Original magnification × 16. (c) Detail of (a). Woven bone present around vascular units. Inset: Fig. 12. DCD nano-particle surface. Original magnification × 16. 677 × 381 mm (72 × 72 DPI).

tissue fraction) in the wound chamber for test and control groups are shown in Table 3. Differences between groups were not statistically significant at any of the time intervals (Fig. 15). Although a higher percentage of bone area was observed at 2 and 4 weeks in the test implant group, bone area results were identical for both groups at the end of the study.

The results from the morphometric measurements of new bone formation (new mineralized tissue fraction) in the wound chamber (thread area) are shown in Table 4. The increase in new bone formation was very similar in both groups (Fig. 16).

The differences in bone area between implant locations (third *versus* fourth premolar site) in the wound chamber (thread area) are represented in Fig. 17. The comparison between $_3P_3$ *versus* $_4P_4$ did not demonstrate statistically significant differences. Nevertheless, in the early healing stage (from 0 to 2 weeks), the third premolar site demonstrated first, bone resorption from 4 h to 1 week and then, bone formation. In contrast, during this period, the distal socket of the fourth premolar demonstrated a slow and continuous new bone formation. After this period (2 weeks), the healing dynamics in both sockets were similar.

The morphometric study of the marginal mirror area (Fig. 18) demonstrated a different healing pattern when third and fourth premolar sites were compared. At the distal socket of the third premolar, bone area dropped from 79.9% (SD 3.1) to 51.5% (SD 13.0) in the interval from 4 h to 1 week, and then there was a rebound towards baseline values from 1–2 weeks of healing. This change was statistically significant ($p \leqslant 0.001$). In contrast, bone density at the fourth premolar site did not experience changes throughout the entire study.

When the healing dynamics were compared between control and test implants, after stratifying by socket location (third and fourth premolar), at the distal socket of the third premolar ($_3P_3$) (Fig. 19a), there was an initial bone resorption from 4 h to 7 days, in both groups, and then, a continuous and gradual bone apposition throughout the entire experimental period. The increase in bone area between 1 and 2 weeks was, however, more pronounced in the test implant group.

At the distal socket of the fourth premolar ($_4P_4$) (Fig. 19b) in the test implant group, the initial bone resorption

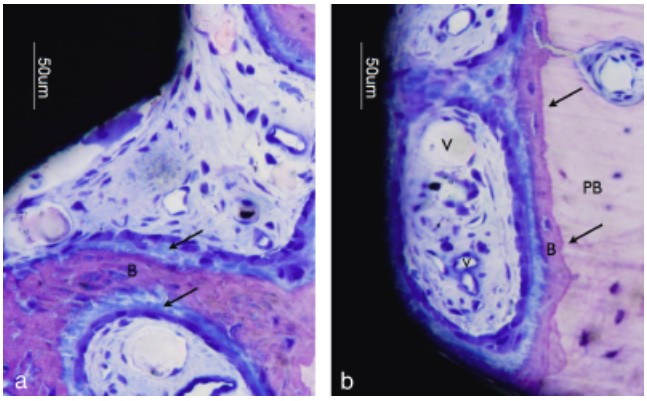

Fig. 12. (a) Osteoblasts lining the bone trabeculae and osteocytes present within the woven bone (B). Osteoid (arrows) separates osteoblasts from the new mineralized tissue (B). (b) Primary osteon forming around vascular units (V). Cement line (arrows) clearly separates the parent bone (PB) from the newly formed bone (B). Toluidine-blue staining. Original magnification × 40. DCD nano-particle surface. z677 × 381 mm (72 × 72 DPI).

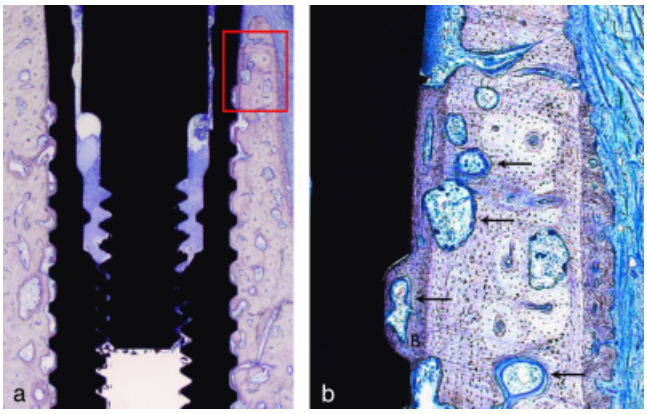

Fig. 13. (a) Implant with surrounding tissues after 4 weeks of healing. Toluidine-blue staining. Original magnification × 10. (b) Detail of (a). Woven bone partly replaced by parallel-fibred bone (B) in contact with the implant surface. Areas of remodelling (arrows) present in the parent bone and in the new bone. Original magnification × 16. DAE surface.

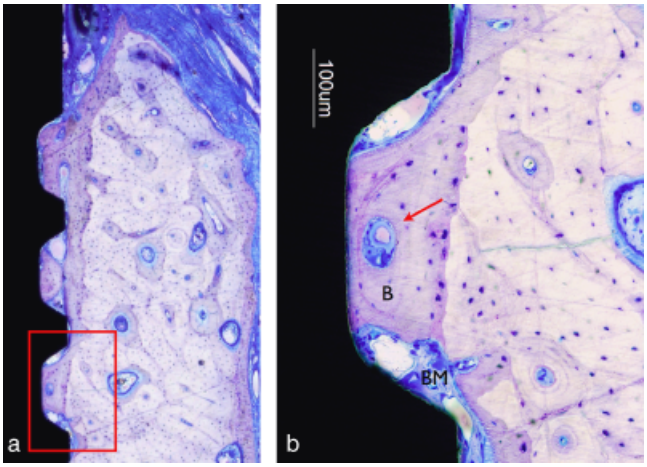

Fig. 14. (a) Ground section representing 8 weeks healing interval. Toluidine-blue staining. Original magnification × 10. (b) Detail of (a). Wound chamber is occupied by mature lamellar bone (B) in intimate contact with the implant surface and also includes areas of bone marrow (BM) in contact with the implant surface. Secondary osteon (arrow). Toluidine-blue staining. Original magnification × 16. 677 × 381 mm (72 × 72 DPI).

from 4 h to 7 days was not observed and bone area demonstrated a continuous and gradual bone apposition throughout the entire experimental period. When new bone formation was calculated for test and control groups, both the percentage and the increase of new bone from 2 to 4 weeks were higher in the test group. At 8 weeks, the amount of new bone formation was similar in both groups (Fig. 20).

Discussion

The biological sequence of bone healing observed in this study is consistent with other reports describing the early phases of wound healing in fresh extraction sockets (Cardaropoli et al. 2003, Araujo & Lindhe 2005) and the healing after inserting an implant in a healed ridge (Berglundh et al. 2003, Abrahamsson et al. 2004). The cascade of events observed in this study started with the formation of a coagulum at 4 h that continued at 1 week with the establishment of a provisional matrix rich in granulation tissue that gradually transformed into woven bone, both in contact with the implant surface and with the parent bone (contact and distance osteogenesis) (Davies 1998). The newly formed woven bone was gradually remodelled into new lamellar bone throughout the study period. Berglundh et al. (2003) designed an experimental wound chamber model to study the wound healing dynamics from 2 h to 120 days after implant placement in healed alveolar ridges. In their study, the first signs of bone resorption were observed at 2 weeks only in the vicinity of parent bone. This finding was also consistent with the results reported by Abrahamsson et al. (2004), which observed a marked reduction of lamellar bone in the same area in the early (1–2 weeks) phases of healing. In this study, bone resorption was first observed at 1 week in both the wound chamber and the marginal mirror area. We have, however, observed differences in healing depending on the socket location, as only the third premolar sites evidenced signs of bone resorption. Measured bone area dropped from 79.9% to 51.5% at the marginal mirror area of third premolar sites, while in contrast, a gradual bone apposition without noticeable resorption, occurred at the fourth premolar sites. These differences are

Table 3. Table shows results from histomorphometric measurements (mean (SD)) of bone area (mineralized tissue fraction) in the wound chamber (thread area)

Bone Area	DAE	Statistics	DCD nanoparticles	Statistics
4 h	34.8 (8.3)		26.0 (8.9)	
1 week	29.2 (10.4)		24.8 (1.4)	
2 weeks	35.8 (13.3)		43.5 (9.7)	
4 weeks	50.2 (3.3)		53.3 (7.4)	
8 weeks	66.3 (9.9)		65.5 (3.4)	

677 × 381 mm (72 × 72 DPI).

P < 0.05
P < 0.01
P < 0.001

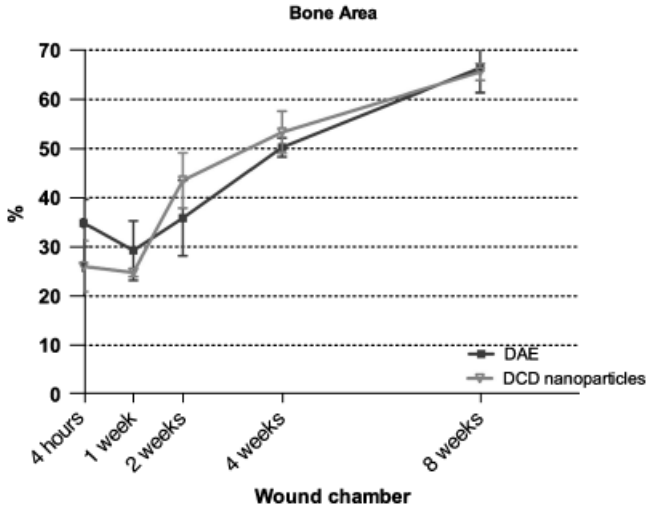

Fig. 15. Bone area (mineralized tissue fraction) in the wound chamber from 4 h to 8 weeks at the DCD nano-particles (red) and DAE (blue) devices. 167 × 143 mm (300 × 300 DPI).

Table 4. Table shows results from histomorphometric measurements (mean (SD)) of new bone formation (new mineralized tissue fraction) in the wound chamber (thread area)

New Bone Formation	DAE	Statistics	DCD nanoparticles	Statistics
4 h	–		–	
1 week	0.9 (1.3)		0.7 (1.0)	
2 weeks	14.2 (7.7)		12.2 (9.0)	
4 weeks	27.0 (8.4)		28.7 (5.0)	
8 weeks	52.3 (3.2)		49.4 (3.2)	

677 × 381 mm (72 × 72 DPI).

P < 0.05
P < 0.01
P < 0.001

probably due to the narrower mesial socket, subject to more surgical trauma by drilling and compression during implant placement. These different healing patterns, however, did not seem to affect the osseointegration process, as there were no differences in BIC percentages between third and fourth premolar sockets at the end of the study.

Further the study aimed to investigate how changes in the implant surface topography at the nano-scale level may influence bone healing and the process of osseointegration. Recent reports have evaluated the ability of nano-topographically complex titanium surfaces to accelerate osseoconduction and to enhance the bone-bonding phenomenon (Williams 1999). With this purpose, different surfaces composed of commercially pure titanium (cpTi) and titanium alloy (Ti6Al4V or Ti64) with microtopographically complex surfaces have been tested. These surfaces were further modified by the DCD of CaP nanoparticles that were able to create a nano-topographic complexity at each implant surface (Mendes et al. 2007, 2008). Findings from these studies in rats evidenced an increase in osseoconduction and a significant enhancement in the bone-bonding phenomenon at the implants with an enhanced surface nano-topography.

In this study, we have evaluated in the beagle dog, the healing of implants with modified surfaces by the DCD of CaP nano-particles and compared it with implants with a standard dual acid-etched surface, when placed immediately in fresh extraction sockets. The enhanced implant surface (DCD) showed higher BIC percentages in the early healing phases (1–4 weeks), although these differences between test and control implants never reached statistical significance. When the bone area was analysed, the test group started with a lower percentage of mineralized tissue in the wound chamber compared with control. However, at 2 and 4 weeks, it rose to higher percentages than the control group. These results are not consistent with those obtained by Meirelles et al. (2007, 2008b) that investigated in the rabbit model the effect of hydroxyapatite nano-particles used to modify smooth titanium implant surfaces. Their results showed statistically significant higher BIC values in the nano-HA enhanced implant surfaces. This discrepancy may be due to the use of smooth-surface implants, *versus* an acid-etched surface used in this investigation. The results in bone area, however, were similar in both studies, as test and control implant surfaces rendered similar outcomes.

Recent studies (Goene et al. 2007, Orsini et al. 2007) have reported human histological and histomorphometric results when evaluating implants placed in the posterior maxilla with an enhanced surface by nanometer-scale CaP added to the dual acid-etched implant surface. In these studies, implants with this enhanced implant surface showed statistically significant higher values of BIC and new bone formation in the early healing stages, when compared with standard acid-etched minimally rough implant surfaces. These findings

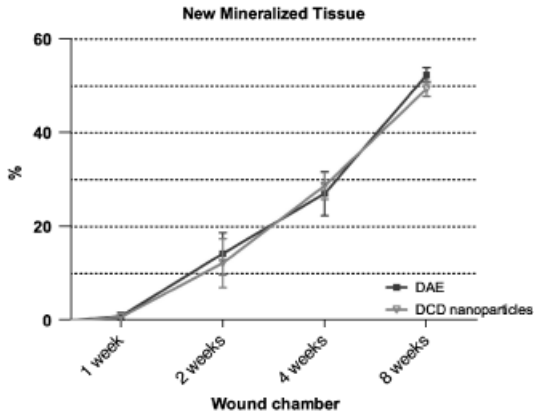

Fig. 16. New bone formation (new mineralized tissue fraction) in the wound chamber from 4 h to 8 weeks at the DCD nano-particles (red) and DAE (blue) devices. 167 × 140 mm (300 × 300 DPI).

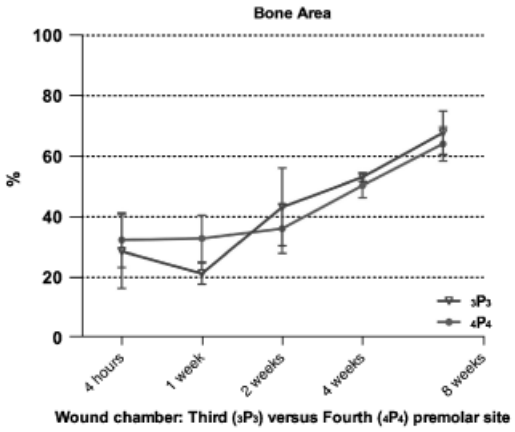

Fig. 17. Bone area (mineralized tissue fraction) from 4 h to 8 weeks at the fourth premolar site (green) and at the third premolar site (purple). Wound chamber. 160 × 144 mm (300 × 300 DPI).

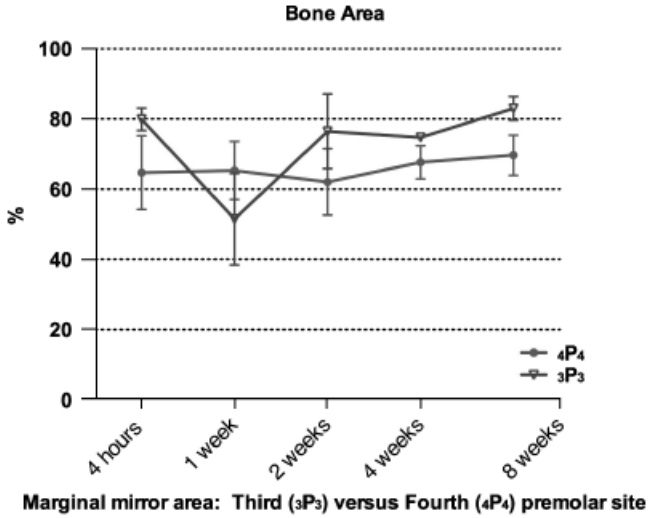

Fig. 18. Bone area (mineralized tissue fraction) from 4 h to 8 weeks at the fourth premolar site (green) and at the third premolar site (purple). Marginal mirror area. 164 × 146 mm (300 × 300 DPI).

are not in agreement with the results obtained in the present investigation in which differences between implants with a different surface nano-topography did not reach statistical significance. Possible reasons for these discrepancies may be the higher bone healing dynamics of the beagle dog that may have masked these differences or the low number of dogs recruited in each group (three in every time interval), which prevented any meaningful statistical analysis. Moreover, the immediate implant surgical protocol used may have jeopardized the potential of the enhanced surface.

We have also assessed whether the socket dimension may influence the healing between implants with different surface nano-topography. Although we did not carry out statistical analysis of the possible differences due to the low number of dogs in each time interval, we could, however, realize that these possible differences were more evident. At the distal socket of the fourth premolar the test implants showed better results in the early healing phases for all the histological outcome variables tested (percentages of BIC, bone area and new bone formation), thus evidencing a faster bone healing dynamic when the space between the implant and the bone was wider. These results are however different from those reported by Meirelles et al. (2008a), in which the effect of hydroxyapatite nano-particles was investigated in a gap-healing model in rabbits and they were not able to demonstrate better results in BIC and bone area at the implants with a surface with nano-particle deposition. This discrepancy may be due to the different experimental model used (artificial defect *versus* implant placement in fresh extraction sockets), or to differences in the implant surface on which the nano-particles were deposited. Furthermore, Meirelles et al. (2008a) modified the implant surface with nano-particles of hydroxyapatite through the sol–gel dip coating process. In this investigation, however, the test implants were modified through the DCD of CAP. Little is known on which is the potential bioactivity of the nano-particles and which is the optimal nano-topography that may influence the healing response. A recent study compared the influence of bio-active and bio-inert nano-structures on bone formation in vivo. Hydroxyapatite (bio-active) and titanium (bio-inert) nano-structures were

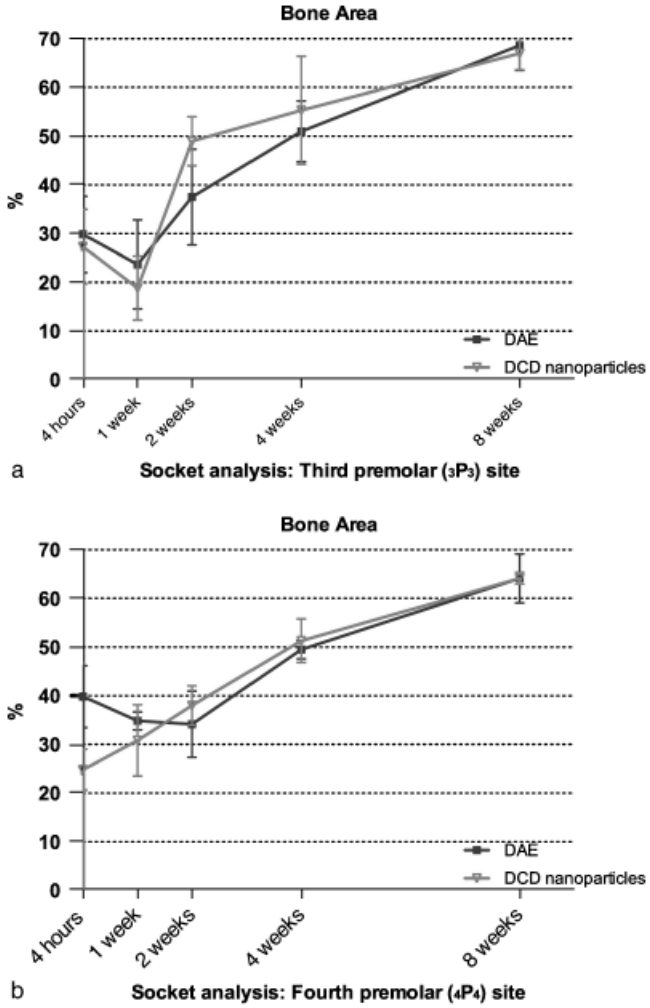

Fig. 19. Bone area (mineralized tissue fraction) from 4 h to 8 weeks at the DCD nano-particles (red) and DAE (blue) devices: (a) third premolar site; (b) fourth premolar site. 168 × 138 mm (300 × 300 DPI).

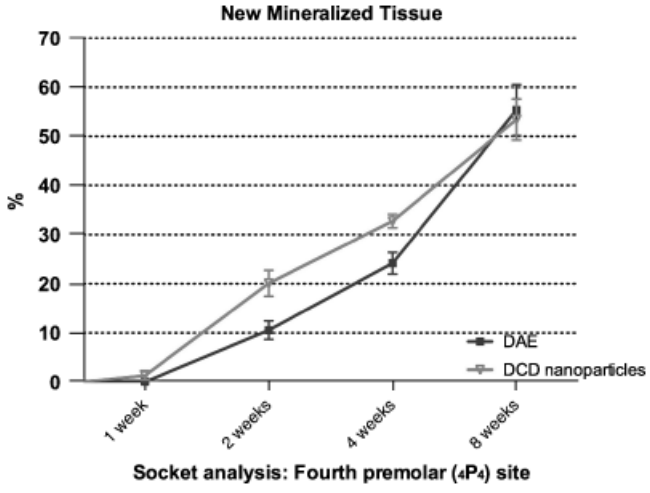

Fig. 20. Fourth premolar site. New bone formation (new mineralized tissue fraction) from 4 h to 8 weeks at the DCD nano-particles (red) and DAE (blue) devices. 167 × 140 mm (300 × 300 DPI).

utilized to modify an electro-polished implant surface. Implants were placed in the rabbit tibia and animals were sacrificed after 4 weeks of healing. BIC measured at titanium implants was higher compared with the HA devices. Authors concluded that these findings did not corroborate the enhanced bone formation to bio-active HA structures and that the higher bone contact was dependent on the nano-feature size and distribution at the surface level (Meirelles et al. 2008c).

In conclusion, bone healing at implants placed into fresh extraction sockets follows a biological cascade of events similar with the wound healing events reported in healed ridges. The process of bone modelling and remodelling appears to be more influenced by the dimension of the socket than the implant surface modification, as bone remodelling was significantly more pronounced at narrower sockets, when implants adapted more intimately to the sockets walls. The DCD demonstrated a discrete influence on the bone healing around implants placed into fresh extraction sockets. At the early healing phases (1–4 weeks), the DCD nano-particles implants (Nanotite™, Biomet 3i) showed higher values of BIC and bone area when compared with DAE surface (Osseotite®, Biomet 3i); however, these differences were not statistically significant and the results were similar in both implant groups at 8 weeks. The effect of the nano-surface implants was more evident when implants were placed in wider sockets, emphasizing the importance of providing a space between the implant and the socket walls for allowing the nano-treated surface to demonstrate a possible positive effect. Future studies should further test this hypothesis and address whether the potential beneficial effect in bone healing may be due to the chemistry of the CaP nano-particles or the nano-topography of the implant surface.

Acknowledgements

We highly appreciate the collaboration of Dr. Giuseppe Cardaropoli who actively participated in the study design and in the implant placement surgeries. We also acknowledge the collaboration of Prof. Peter Thomsen who participated in the histological processing of this material.

References

Abrahamsson, I., Berglundh, T., Linder, E., Lang, N. P. & Lindhe, J. (2004) Early bone formation adjacent to rough and turned endosseous implant surfaces. An experimental study in the dog. *Clinical Oral Implants Research* **15**, 381–392.

Albrektsson, T., Branemark, P. I., Hansson, H. A. & Lindström, J. (1981) Osseointegrated titanium implants. Requirements for ensuring a long-lasting direct bone-to-implant anchorage in man. *Acta Orthopaedica Scandinavica* **52**, 155–170.

Anneroth, G., Hedstrom, K. G., Kjellman, O., Kondell, P. A. & Nordenram, A. (1985) Endosseus titanium implants in extraction sockets. An experimental study in monkeys. *International Journal of Oral Surgery* **14**, 50–54.

Araujo, M. G. & Lindhe, J. (2005) Dimensional ridge alterations following tooth extraction. An experimental study in the dog. *Journal of Clinical Periodontology* **32**, 212–218.

Araujo, M. G., Sukekava, F., Wennstrom, J. L. & Lindhe, J. (2005) Ridge alterations following implant placement in fresh extraction sockets: an experimental study in the dog. *Journal of Clinical Periodontology* **32**, 645–652.

Araujo, M. G., Sukekava, F., Wennstrom, J. L. & Lindhe, J. (2006a) Tissue modeling following implant placement in fresh extraction sockets. *Clinical Oral Implants Research* **17**, 615–624.

Araujo, M. G., Wennstrom, J. L. & Lindhe, J. (2006b) Modeling of the buccal and lingual bone walls of fresh extraction sites following implant installation. *Clinical Oral Implants Research* **17**, 606–614.

Barzilay, I., Graser, G. N., Iranpour, B. & Natiella, J. R. (1991) Immediate implantation of a pure titanium implant into an extraction socket: report of a pilot procedure. *International Journal of Oral & Maxillofacial Implants* **6**, 277–284.

Berglundh, T., Abrahamsson, I., Lang, N. P. & Lindhe, J. (2003) De novo alveolar bone formation adjacent to endosseous implants. *Clinical Oral Implants Research* **14**, 251–262.

Blanco, J., Nunez, V., Aracil, L., Munoz, F. & Ramos, I. (2008) Ridge alterations following immediate implant placement in the dog: flap versus flapless surgery. *Journal of Clinical Periodontology* **35**, 640–648.

Botticelli, D., Persson, L. G., Lindhe, J. & Berglundh, T. (2006) Bone tissue formation adjacent to implants placed in fresh extraction sockets: an experimental study in dogs. *Clinical Oral Implants Research* **17**, 351–358.

Cardaropoli, G., Araujo, M. & Lindhe, J. (2003) Dynamics of bone tissue formation in tooth extraction sites. An experimental study in dogs. *Journal of Clinical Periodontology* **30**, 809–818.

Davies, J. E. (1998) Mechanisms of endosseous integration. *International Journal of Prosthodontics* **11**, 391–341.

Donath, K. & Breuner, G. (1982) A method for the study of undecalcified bones and teeth with attached soft tissues. The Sage-Schliff (sawing and grinding) technique. *Journal of Oral Pathology* **11**, 318–326.

Goene, R. J., Testori, T. & Trisi, P. (2007) Influence of a nanometer-scale surface enhancement on de novo bone formation on titanium implants: a histomorphometric study in human maxillae. *The International Journal of Periodontics & Restorative Dentistry* **27**, 211–219.

Johansson, C. & Albrektsson, T. (1987) Integration of screw implants in the rabbit: a1-year follow-up removal torque of titanium implants. *Int J Oral Maxillofac Implants* 1987 Spring; **2** (2), 69–75.

Johansson, C. (1991) On Tissue Reactions to Metal Implants. PhD Thesis, Biomaterials Group, Department of Handicap Research, University of Goteborg, Goteborg, Sweden.

Karnovsky, M. J. (1965) A formaldehyde–glutaraldehyde fixative of high osmolarity for use in electron microscopy. *Journal of Cell Biology* **27**, 137A–138A.

Meirelles, L., Albrektsson, T., Kjellin, P., Arvidsson, A., Franke-Stenport, V., Andersson, M., Currie, F. & Wennerberg, A. (2008a) Bone reaction to nano hydroxyapatite modified titanium implants placed in a gap-healing model. *Journal of Biomedical Materials Research A* **87**, 624–631.

Meirelles, L., Arvidsson, A., Albrektsson, T. & Wennerberg, A. (2007) Increased bone formation to unstable nano rough titanium implants. *Clinical Oral Implants Research* **18**, 326–332.

Meirelles, L., Arvidsson, A., Andersson, M., Kjellin, P., Albrektsson, T. & Wennerberg, A. (2008b) Nano hydroxyapatite structures influence early bone formation. *Journal of Biomedical Materials Research A* **87**, 299–307.

Meirelles, L., Melin, L., Peltola, T., Kjellin, P., Kangasniemi, I., Currie, F., Andersson, M., Albrektsson, T. & Wennerberg, A. (2008c) Effect of hydroxyapatite and titania nanostructures on early in vivo bone response. *Clinical Implant Dentistry and Related Research* **10**, 245–254.

Mendes, V. C., Moineddin, R. & Davies, J. E. (2007) The effect of discrete calcium phosphate nanocrystals on bone-bonding to titanium surfaces. *Biomaterials* **28**, 4748–4755.

Mendes, V. C., Moineddin, R. & Davies, J. E. (2008) Discrete calcium phosphate nanocrystalline deposition enhances osteoconduction on titanium-based implant surfaces. *Journal of Biomedical Materials Research A*. June 18 [Epub ahead of print].

Orsini, G., Piattelli, M., Scarano, A., Petrone, G., Kenealy, J., Piattelli, A. & Caputi, S. (2007) Randomized, controlled histologic and histomorphometric evaluation of implants with nanometer-scale calcium phosphate added to the dual acid-etched surface in the human posterior maxilla. *Journal of Periodontology* **78**, 209–218.

Rimondini, L., Bruschi, G. B., Scipioni, A., Carrassi, A., Nicoli-Aldini, N., Giavaresi, G., Fini, M., Mortellaro, C. & Giardino, R. (2005) Tissue healing in implants immediately placed into postextraction sockets: a pilot study in a mini-pig model. *Oral Surgery, Oral Medicine, Oral Pathology, Oral Radiology, and Endodontics* **100**, e43–e50.

Schroeder, A., Van der Zypen, E., Stich, H. & Sutter, F. (1981) the reaction of bone, connective tissue, and epithelium to endosteal implants with titanium-sprayed surfaces. *Journal of Maxillofacial Surgery Feb* **9**, 15–25.

Schropp, L., Kostopoulos, L. & Wenzel, A. (2003) Bone healing following immediate versus delayed placement of titanium implants into extraction sockets: a prospective clinical study. *International Journal of Oral & Maxillofacial Implants* **18**, 189–199.

Todescan, R. Jr., Pilliar, R. M. & Melcher, A. H. (1987) A small animal model for investigating endosseous dental implants: effect of graft materials on healing of endosseous, porous-surfaced implants placed in a fresh extraction socket. *International Journal of Oral & Maxillofacial Implants* **2**, 217–223.

Wennerberg, A., Albrektsson, T. & Andersson, B. (1996a) Bone tissue response to commercially pure titanium implants blasted with fine and coarse particles of aluminum oxide. *International Journal of Oral & Maxillofacial Implants* **11**, 38–45.

Wennerberg, A., Albrektsson, T., Andersson, B. & Krol, J. J. (1995) A histomorphometric and removal torque study of screw-shaped titanium implants with three different surface topographies. *Clinical Oral Implants Research* **6**, 24–30.

Wennerberg, A., Albrektsson, T., Johansson, C. & Andersson, B. (1996b) Experimental study of turned and grit-blasted screw-shaped implants with special emphasis on effects of blasting material and surface topography. *Biomaterials* **17**, 15–22.

Wennerberg, A., Albrektsson, T. & Lausmaa, J. (1996c) Torque and histomorphometric evaluation of c.p. titanium screws blasted with 25- and 75-microns-sized particles of Al_2O_3. *Journal of Biomedical Materials Research* **30**, 251–260.

Williams, D. (1999) *The Williams Dictionary of Biomaterials*. Liverpool: Liverpool University Press.

Address:
Fabio Vignoletti
Universidad Complutense de Madrid
Periodoncia
Madrid
Spain
E-mail: fabiovignoletti@mac.com

Clinical Relevance

Scientific rationale for the study: Immediate implant installation at fresh extraction sockets is a surgical protocol commonly used in clinical practice. Limited information is available on: (i) the early process of tissue integration, (ii) its predictability and (iii) whether implants with improved surface nano-topography may influence this process. It is, therefore, relevant to identify the biological sequence of healing during the early phases of osseointegration using this surgical protocol.

Principal findings: Immediate implant installation into an extraction socket elicits a cascade of biological events including necrosis due to surgical trauma, bone resorption and a concomitant process of new bone formation. This process of bone modelling and remodelling is influenced by the dimension of the socket, being significantly more pronounced when implants adapt more intimately to the sockets walls. Improved implant surfaces by nano-sized crystalline deposition had a limited added effect of on bone healing, however, this was more evident at the wider forth-premolar sites.

Practical implications: When there is a close adaptation between the implant surface and the socket wall we may expect more bone resorption probably due to trauma from drilling and implant compression. Enhanced implant surfaces may improve bone dynamics when a wider void occurs between the implant surface and the socket walls.